Analytic approach for optimal quantization of diffractive optical elements

Uriel Levy, Nadav Cohen, and David Mendlovic

One of the most important factors that limit the performance of diffractive optical elements (DOE's) is the depth accuracy of the relief structure. A common procedure for fabricating DOE's is the binary optics procedure, in which binary masks are used for the fabrication of a multilevel relief structure. Here an analytic procedure for calculating the optimal depth levels of DOE's, the phase bias, and the decision levels is presented. This approach is based on the minimization of the mean-squared error caused by the quantization of the continuous profile. As a result of the minimization an optimal value for the etching depth of each photolithographic mask is determined. The obtained depth values are, in general, different from the depth values used by the conventional multilevel approach. Comprehensive mathematical analysis is given, followed by several computer simulations that demonstrate the advantages of the proposed procedure. © 1999 Optical Society of America

OCIS codes: 050.1970, 050.1380.

1. Introduction

Diffractive optical elements (DOE's) play a major role in various applications such as beam shaping,[1] optical data processing,[2] optical interconnection,[3] and others. These elements are mainly based on a surface relief pattern and thus possess several advantages. Mainly, these include their high light efficiency, which is obtained by not using absorptive material. The above DOE's are used to describe a continuous phase profile, which may contain any desired information. DOE's can be fabricated by use of several approaches.

A promising approach for the fabrication of continuous phase profiles is direct laser beam writing. According to this approach the substrate is exposed to an UV laser beam that is focused on the substrate. Substrate scanning is achieved with an *x*–*y* translator, which moves the beam or, alternatively, the surface itself. At each location the intensity exposure is controlled according to the desired depth. The substrate is usually coated with photoresist,[4] although writing directly onto the substrate is also possible (laser ablation).[5,6] Another direct writing approach is electron beam writing.[7,8] Direct writing techniques, although they seem quite promising, suffer from several disadvantages, mainly the long fabrication period and the complexity of the systems.

Diamond turning is based on a programmable machining technique, which makes use of a machine and a cutting tool to obtain continuous phase profiles with minimal roughness.[9] However, this approach is limited to low numerical apertures (NA's) and rotationally symmetric elements. Moreover, the implementation of this method by use of a glass substrate is difficult, because glass is a brittle material.

Owing to the above limitations, the common approach for the fabrication of DOE's is still by use of a multilevel phase profile.[10] This approach is known as binary optics. The approach is based on producing a set of binary masks and performing etching steps for achieving a phase delay of π (first mask), $\pi/2$ (second mask), $\pi/4$ (third mask), and so on. Usually, no more than four masks are used; therefore $2^4 = 16$ phase levels are achieved. The continuous phase profile is approximated by the quantized profile with the aid of binary masks. The quantized phase levels are equally spaced in the $[0-2\pi]$ span.

Before we discuss optimal etching-depth levels, it is important to note that, even for the ideal case of an infinite number of lithographic masks, one cannot obtain a continuous phase profile, owing to the spatial sampling. For example, the implementation of a high-NA lens with a low space–bandwidth product

---

The authors are with the Faculty of Engineering, Tel Aviv University, 69978 Tel Aviv, Israel. D. Mendlovic's e-mail address is mend@eng.tau.ac.il.

Received 24 February 1999; revised manuscript received 26 May 1999.

0003-6935/99/265527-06$15.00/0

DOE leads to significant phase quantization. In such cases optimization should be based on proper design of the lithographic masks. Several approaches to this type of optimization can be found in the literature.[11–13]

In this paper we investigate cases in which phase quantization is governed by the number of lithographic masks rather than by the space–bandwidth product. DOE's for arbitrary beam shaping and low NA are examples for such a case. Under this assumption the uniform set of etching-depth levels, although commonly used, is optimal only for a limited set of cases in which the phase probability-density function is constant (i.e., equal number of pixels per each phase region), such as linear phase (blazed grating). However, if the phase probability-density function is not constant, e.g., a Fresnel lens, another set of etching depths may describe more accurately the continuous phase profile. Controlling the phase bias may also be helpful, as shown by Hen and Sawchuk.[14] An iterative approach for obtaining the optimal etching-depth levels as well as the phase bias was presented by Arrizon and Sinzinger.[15] The approach is based on defining a criterion for optimization and performs numerical gradient optimization. Using the above approach, the authors succeeded in obtaining array generators with higher uniformity. The approach has several advantages, such as the ability to define any desired criterion for optimization. However, finding an analytic expression (rather than a numerical one) that defines the optimal etching-depth levels and the phase bias is crucial, from both academic and calculation complexity points of view. In addition, the above approach assumes that the decision levels lie exactly in the middle of a region defined by two consecutive phase levels. This assumption, although it seems quite reasonable, is worth checking. Therefore we aim to find an analytic expression for the optimal etching-depth levels.

When trying to find an analytic expression for optimal quantization, one usually refers to the well-known Max–Lloyd algorithm.[16,17] This algorithm yields the optimal gray levels for quantizing an image. Unfortunately, that algorithm in its known form is not suitable for quantizing a continuous phase profile, for to two reasons:

1. The quantization should optimize a phasor (which is a periodic function with period of 2π) rather than gray-scale levels.
2. When the binary optics manufacturing procedure is used, the phase values are a function of the etching-depth levels and therefore cannot be chosen arbitrarily as are gray-scale levels. As a result, fewer degrees of freedom exist.

An analytic approach for calculating the optimal quantization of computer-generated holograms was suggested by Gallagher.[18] This approach is based on the Max–Lloyd algorithm and finds both amplitude and phase quantization levels. Suitable constraints are used to apply the approach to Lohmann and Lee computer-generated holograms. However, the above constraints are not suitable for the optimization of phase-only DOE's fabricated with the concept of binary optics.

In the following an approach for calculating the optimal etching depths analytically is presented. The proposed approach is based on the Max–Lloyd optimization. It is applied to the optimization of phase-only DOE's fabricated with the binary optics technique, by the introduction of proper constraints. Based on knowledge of the phase probability-density function, the optimal phase profile can be found by the minimization of the mean-squared error (MSE) term. A comprehensive mathematical analysis is given in Section 2. Computer simulations are given in Section 3, and in Section 4 we summarize and conclude the results.

2. Mathematical Analysis

The quantization operation yields some error, which is known as quantization noise. Our aim is to find a set of etching-depth levels, $d_1, \ldots, d_N$ (where N is the number of desired lithographic masks and d is given in phase units), a hard-clipping set $C_1, \ldots, C_{N+1}$ (where C_j, C_{j+1} defines the region of allocating a continuous phase ϕ into a quantized phase ϕ_j), and a reference quantized phase ϕ_1 (phase bias), all of which minimize the MSE given by

$$E = \sum_{l=1}^{l=2^N} \int_{C_l}^{C_{l+1}} |\exp(i\phi) - \exp(i\phi_l)|^2 p(\phi) \mathrm{d}\phi, \tag{1}$$

where $p(\phi)$ is the probability density of ϕ. We can find the minimization conditions by differentiating Eq. (1) with respect to C_m, d_r, and ϕ_1 and equating to zero. As a result the following set of equations is obtained:

$$\frac{\partial E}{\partial C_m} = |\exp(iC_m) - \exp(i\phi_{m-1})|^2 p(\phi_m) - |\exp(iC_m) - \exp(i\phi_m)|^2 p(\phi_m) = 0, \tag{2}$$

$$\frac{\partial E}{\partial d_r} = \sum_{n=1}^{2^N} \frac{\partial E}{\partial \phi_n} \frac{\partial \phi_n}{\partial d_r} = \sum_{n=1}^{2^N} \int_{C_n}^{C_{n+1}} \sin(\phi - \phi_n) \times p(\phi) \frac{\partial \phi}{\partial d_r} \mathrm{d}\phi = 0, \tag{3}$$

$$\frac{\partial E}{\partial \phi_1} = \int_{C_1}^{C_2} \sin(\phi - \phi_1) p(\phi) \mathrm{d}\phi = 0, \tag{4}$$

By applying some simple mathematical manipulations on Eq. (2), one gets

$$C_m = (\phi_m + \phi_{m-1})/2, \tag{5}$$

which is similar to the results obtained with the Max–Lloyd algorithm. Before substituting the above results into Eqs. (3) and (4) and obtaining a solution for the set d_r and for ϕ_1, one must know the analytic dependence of ϕ_n in d_r. The general expression for this dependence is given by

$$\phi_n = \phi_1 + \sum_{r=1}^{N} d_r \sum_{p=1}^{2^{r-1}} \sum_{j=2N-r+1}^{2^{N-r+1}} \delta_{n,j+(p-1)2^{N-r+1}}, \qquad (6)$$

where $\delta_{i,j}$ is the discrete Kronecker delta function, defined as

$$\delta_{i,j} = \begin{cases} 1 \text{ if } i = j \\ 0 \text{ if } i \neq j \end{cases}. \qquad (7)$$

The various masks usually conform to the simple relation

$$d_r > \sum_{j=r+1}^{N} d_j, \ldots, 1 < r < N-1. \qquad (8)$$

For masks that fulfill condition (8), Eq. (6) may be formulated more simply as an inner product:

$$\phi_n = \phi_1 + (n-1)_{N,2} \cdot (d_1, d_2, \ldots, d_N)^t, \qquad (9)$$

where $(n-1)_{N,2}$ is the N-digit binary vector representation of $n-1$, $\cdot$ is the inner product, and t is the transpose operation.

Although Eq. (6) is somewhat complicated, it is easy to obtain the matrix $\partial\phi_n/\partial d_r$. As an example, we discuss the case of $N = 2$, i.e., two masks and $2^2 = 4$ phase levels. From Eq. (6) one obtains

$$\phi_1 = \phi_1, \qquad \phi_2 = \phi_1 + d_2, \qquad \phi_3 = \phi_1 + d_1,$$
$$\phi_4 = \phi_1 + d_1 + d_2; \qquad (10)$$

therefore

$$\frac{\partial\phi_n}{\partial d_r} = \begin{bmatrix} 0 & 0 \\ 0 & 1 \\ 1 & 0 \\ 1 & 1 \end{bmatrix}, \qquad (11)$$

where r is the column index and n is the row index.

Extreme phase levels pose an additional problem. As can be seen from Eq. (5), finding C_1 and C_{N+1} involves expressions with ϕ_0, ϕ_{N+1}, which are not defined. However, bearing in mind that ϕ is a phasor and thus should be a periodic function with 2π periodicity, we must define $\phi_0 = \phi_N - 2\pi$, $\phi_{N+1} = \phi_1 + 2\pi$. An integral whose boundaries cross 2π (e.g., an integral with boundaries $[1.9\pi$–$0.1\pi]$) should be replaced with two integrals: from the lower boundary up to 2π and from 0 up to the upper limit, e.g., from 1.9π to 2π and from 0 to 0.1π, respectively. Integrals of this type may result either from $\phi_{N+1} > 2\pi$ (causing boundaries such as 1.9π–2.1π) or from $\phi_0 < 0$ (causing boundaries such as -0.1π–0.1π).

Table 1. Optimal Etching Depth Levels for the Fabrication of the $F = 8$ m Fresnel Lens

	ϕ_1	d_1	d_2	d_3
$N = 1$	0.63	2.958		
$N = 2$	0.181	3.0159	1.4608	
$N = 3$	0.1	3.0788	1.5237	0.7461

It is still necessary to obtain an expression for $p(\phi)$. It is convenient to perform this task with a computer, by means of dividing the phase region $[0$–$2\pi]$ into a large number of discrete partitions, counting the number of pixels that belong to each partition, and performing normalization. If, however, the phase profile is given as an analytic function, it is also possible to find $p(\phi)$ analytically. Assuming that the dependence of ϕ in the spatial location x (which is distributed uniformly) is given by $\phi(x) = f(x)$, it can be shown that

$$p(\phi) = \text{const}\,\frac{\mathrm{d}x}{\mathrm{d}\phi}. \qquad (12)$$

Although the constant can be found by normalization, it can be neglected, owing to the structure of Eqs. (3) and (4) (const[. . .] = 0).

The next step is substituting Eqs. (5) and (6) into Eqs. (3) and (4). Equation (3) is a set of N nonlinear equations; therefore the $N + 1$ unknown parameters $[d_1, \ldots, d_N, \phi_1]$ can be found from the above equations. Note that, although every equation is a sum of 2^N terms, only half of the phase levels are dependent on d_r. Therefore only 2^{N-1} terms remain, which makes the calculations easier. For the case of a large number of lithographic masks, (i.e., large N) the term $\phi - \phi_n$ becomes small; therefore the approximation

$$\sin(\phi - \phi_n) \approx (\phi - \phi_n) \qquad (13)$$

is valid. Using the above approximation leads to simpler equations, which are easier to solve. However, where large N values are involved, the improvement of the proposed approach becomes less significant. Thus using the approximation of relation (13) might cancel the error reduction, and the exact solution is preferable.

3. Computer Simulations

To demonstrate the advantages of the presented approach, several computer simulations were carried out. The first case that was investigated is the multilevel Fresnel lens, also known as the zone plate. We used a weak Fresnel lens with an aperture of 6.3 mm and focal length of 8 m, designed for a wavelength of 0.632 μm. The suggested algorithm was used to find the set $(d_1, \ldots, d_N, \phi_1)$ for $N = 1, 2, 3$. The obtained results are given in Table 1 (The continuous, uniform-quantized, and nonuniform-quantized profiles can bee seen in Fig. 1). MSE values are presented in Table 2. No significant improvement was achieved using with three masks; therefore these results are not given.

Although the above approach is based on optimization of the MSE, the evaluation of the quantized lens performances should be based on an energy criterion. Even though MSE improvement does not necessarily lead to efficiency improvement. It is in-

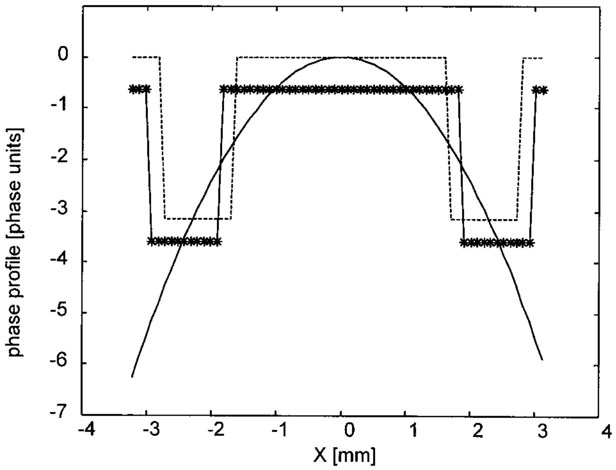

Fig. 1. Continuous (solid curve), uniform-binary-quantized (dashed line), and nonuniform-binary-quantized (curve with asterisks) lens profiles.

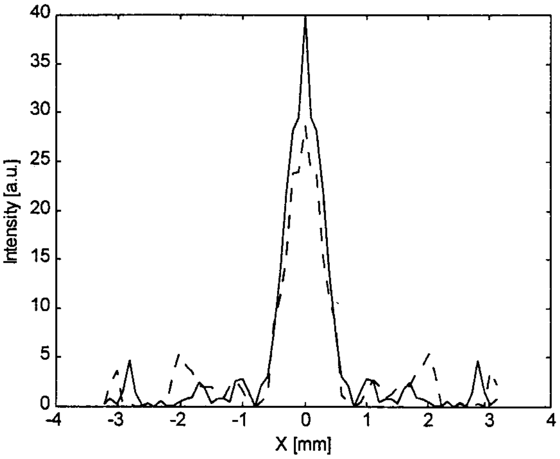

Fig. 2. Image cross section at the focal plane, obtained with the uniform- (dashed curve) and the nonuniform- (solid curve) binary-quantized lenses.

Table 2. Obtained MSE and Efficiency Values for the *F* = 8 m Fresnel Lens

	Nonuniform MSE	Uniform MSE	Nonuniform Efficiency (%)	Uniform Efficiency (%)	MSE Improv. (%)	Efficiency Improv. (%)
$N = 1$	0.68	0.71	48.6	40.5	4.4	20
$N = 2$	0.195	0.199	82.7	81	2.6	2

teresting to examine how the nonuniform quantization influences the energy distribution at the focal plane. We calculated the energy inside the central lobe of the of the lens and compared that with the expected values for the uniform-quantized lens[19]:

$$\eta_N = \left|\mathrm{sinc}\left(\frac{1}{2^N}\right)\right|^2. \tag{14}$$

The results for the first two masks are also given in Table 2. Significant improvement was obtained only for the binary lens ($N = 1$), efficiency of 48.6% instead of 40.5%. The cross section of the image at the focal plane, obtained with the uniform- and the nonuniform-binary-quantized lenses are depicted in Fig. 2. The obtained MSE values are given in Table 2.

Another case that was investigated is a Fresnel lens with a focal length of 5 m and an aperture of 6.2 mm. The parameters of this lens were chosen such that the phase variations are from 0 to 3π. Because of the periodicity, the phase region 2π–3π is folded into the 0–π region. Therefore most of the phase values are concentrated in this region, and it seems that nonuniform quantization may be quite helpful. The suggested algorithm was used to find the set ($d_1, \ldots, d_N, \phi_1$) for $N = 1, 2, 3$. The obtained results are given in Table 3 (the continuous, uniform-quantized, and nonuniform-quantized profiles can be seen in Fig. 3). MSE values are presented in Table 4. As expected, MSE improvement is more significant compared with the 8-m lens, although the efficiency improvement is less impressive.

Table 3. Optimal Etching Depth Levels for the Fabrication of the *F* = 5 m Fresnel Lens

	ϕ_1	d_1	d_2	d_3
$N = 1$	0.660	2.832		
$N = 2$	0.231	3.014	1.524	
$N = 3$	0.315	3.105	1.515	0.766

To emphasize the capabilities of the proposed approach, a phase-only filter that reconstructs the letter

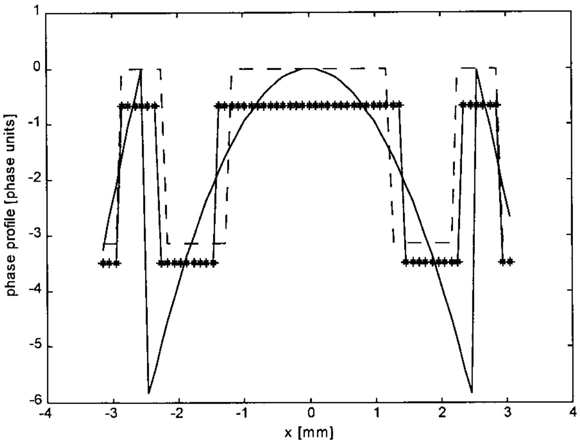

Fig. 3. Continuous (solid curve), uniform-binary-quantized (dashed line), and nonuniform-binary-quantized (curve with asterisks) lens ($F = 5$ m) profiles.

Table 4. Obtained MSE and Efficiency Values for the F = 5 m Fresnel Lens

	Nonuniform MSE	Uniform MSE	Nonuniform Efficiency (%)	Uniform Efficiency (%)	MSE Improv. (%)	Efficiency Improv. (%)
$N = 1$	0.684	0.721	45.9	40.5	5.4	13.3
$N = 2$	0.192	0.198	82.5	81	3.2	1.85
$N = 3$	0.0496	0.0511	95	95	3	None

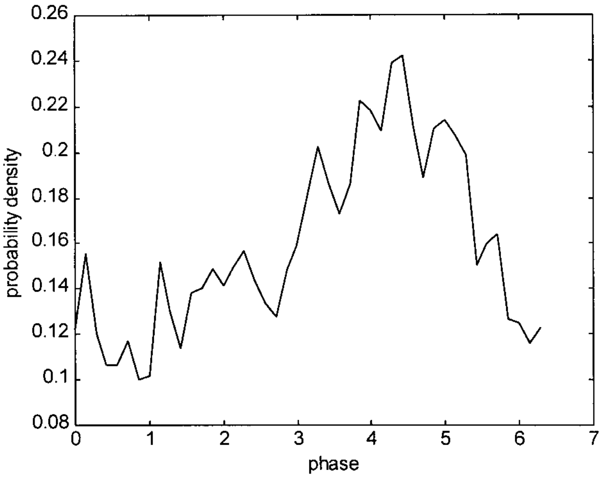

Fig. 4. Probability-density function for the L DOE.

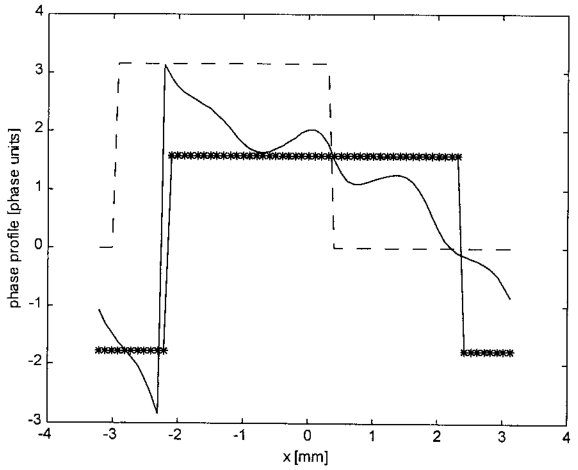

Fig. 5. Continuous (solid curve), uniform-binary-quantized (dashed line), and nonuniform-binary-quantized (curve with asterisks) profiles of the L DOE.

L was designed (with the Gerchberg–Saxton algorithm[20]). The probability-density function, which can be seen in Fig. 4, was calculated. The obtained values for $\phi_1, d_1, \ldots, d_N$ are given in Table 5. The obtained MSE values are given in Table 6. The continuous, uniform-quantized, and nonuniform-quantized profiles can be seen in Fig. 5.

As can be seen, significant improvement is obtained for the binary DOE, whereas the improvement decreases with the increase of N. Nevertheless, even a 2–3% improvement cannot be underestimated, and sometimes it can make a significant difference, especially since no additional fabrication effort is needed.

Table 5. Optimal Etching Depth Levels for the Fabrication of the L DOE

	ϕ_1	d_1	d_2	d_3
$N = 1$	1.574	2.939		
$N = 2$	0.410	3.086	1.538	
$N = 3$	0.930	3.145	1.563	0.785

Table 6. Obtained MSE Values for the L DOE

	Nonuniform MSE	Uniform MSE	Improv. (%)
$N = 1$	0.6759	0.7674	13.54
$N = 2$	0.1914	0.1978	3.34
$N = 3$	0.0500	0.0513	2.60

4. Conclusions

A novel, to our knowledge, method that enables analytical calculation of the optimal etching-depth levels, the phase bias, and the decision levels has been presented. These etching-depth levels, combined with appropriate masks, can be used for the fabrication of multilevel DOE's. It was shown that the decision levels lie exactly between two consecutive phase values. It was also shown that the error caused by the quantization could be reduced with the suggested approach. Three different DOE's were tested: two Fresnel lenses ($F = 8$ m and $F = 5$ m) and a phase-only filter that reconstructs the letter L. The quantization error was significantly reduced for the first two etching levels of all the three DOE's, whereas for the case of three masks error reduction can be noticed on the Fresnel lens with a focal length of 5 m and on the L filter. In general, the approach is useful especially for binary elements but may also be helpful for multilevel elements.

The authors thank the Israeli Ministry of Science and the Arts for its support in the framework of the National Infrastructure program. Uriel Levy and Nadav Cohen thank the Israeli Ministry of Science and the Arts for the Eshkol fellowship.

References

1. F. Wyrowski and O. Bryngdahl, "Iterative Fourier transform algorithm applied to computer holography," J. Opt. Soc. Am A **7,** 961–969 (1988).

2. J. L Horner and J. R. Leger, “Pattern recognition with binary phase-only filters,” Appl. Opt. **24,** 609–611 (1985).
3. S. J. Walker and J. Jahns, “Optical clock distribution using integrated free-space optics,” Opt. Commun. **90,** 359–371 (1992).
4. M. T. Gale, M. Rossi, J. Pederson, and H. Schutz, “Fabrication of continuous-relief micro-optical elements by direct laser writing in photoresist,” Opt. Eng. **33,** 3556–3566 (1994).
5. H. M. Phillips and R. A. Sauerbrey, “Eximer-laser-produced nanostructures in polymers,” Opt. Eng. **32,** 2424–2436 (1993).
6. N. A. Vainos, S. Mailis, S. Pissadakis, L. Boutsikaris, P. J. M. Parmiter, P. Dainty, and T. J. Hall, “Excimer laser use for microetching computer-generated holographic structures,” Appl. Opt. **35,** 6304–6319 (1996).
7. M. Ekberg, M. Larsson, S. Hard, and B. Nilsson, “Multilevel phase holograms manufactured by electron-beam lithography,” Opt. Lett. **15,** 568–569 (1990).
8. M. Larsson, M. Ekberg, F. Nikolajeff, and S. Hard, “Successive-development optimization of resist kinoforms manufactured with direct writing, electron-beam lithography,” Appl. Opt. **33,** 1176–1179 (1994).
9. H. P. Herzig, *Micro-optics: Elements, Systems and Applications* (Taylor & Francis, London, 1997).
10. G. J. Swanson and W. B. Weldkamp, “High-efficiency, multilevel, diffractive optical elements,” US. patent 4,895,790 (23 January 1987).
11. W. H. Welch, J. E. Morris, and M. R. Feldman, “Iterative discrete on-axis encoding of radially symmetric computer-generated holograms,” J. Opt. Soc. Am. A **10,** 1729–1738 (1993).
12. M. Kuittinen and H. P. Herzig, “Encoding of efficient diffractive microlenses,” Opt. Lett. **20,** 2156–2158 (1995).
13. J. Fan, D. Zaleta, K. S. Urquhart, and S. H. Lee, “Efficient encoding algorithms for computer-aided design of diffractive optical elements by the use of electron-beam fabrication,” Appl. Opt. **34,** 2522–2533 (1995).
14. C. Chen and A. A. Sawchuk, “Nonlinear least-squares and phase-shifting quantization methods for diffractive optical element design,” Appl. Opt. **36,** 7297–7306 (1997).
15. V. Arrizon and S. Sinzinger, “Modified quantization schems for Fourier-type array generator,” Opt. Commun. **140,** 309–315 (1997).
16. A. K. Jain, *Fundamentals of Digital Image Processing* (Prentice-Hall Engelwood Cliffs, N.J., 1989).
17. J. Max, “Quantizing for minimum distortion,” IEEE Trans. Inf. Theory **IT-6,** 7–12 (1960).
18. N. C. Gallagher, “Optimum quantization in digital holography,” Appl. Opt. **17,** 109–115 (1978).
19. G. J. Swanson and W. B. Weldkamp, “Diffractive optical elements for use in infrared systems,” Opt. Eng. **28,** 605–608 (1989).
20. R. W. Gerchberg and W. O. Saxton, “A practical algorithm for the determination of phase from image and diffraction plane pictures,” Optik **35,** 237–246 (1972).